Proceedings of the ASPF 2003 (The 8th Asian Symposium on Precision Forging), October 15 - 18, 2003

FE ANALYSIS OF INTERFACIAL BEHAVIOR OF COLD FORGING TOOL COATED BY HARD FILM

Kunio HAYAKAWA

Department of Mechanical Engineering, Shizuoka University
3-5-1 Johoku, Hamamatsu, 432-8561, Japan
tmkhaya@ipc.shizuoka.ac.jp

Abstract

A behavior of interface of cold forging tool coated by hard film is analyzed by FEM. The indentation of a hemispherical tool of SUJ2 in JIS coated by electroplated coating of chromium into a cylindrical workpiece of S25C in JIS is performed. The proposed constitutive equations are implemented by the non-linear springs model at the interface. Calculated results show that the maximum interfacial normal displacement is observed at an immediately forward from the lip of the indentation, whereas maximum interfacial tangential displacement is at the immediately backward of the lip of the indentation.

Key words: Interface, Damage, Cold Forging, Tool, Hard film, Debonding.

1. Introduction

Recently, forging tools coated by hard films such as electroplated coating of chromium, TiN, TiC and so on, are used aiming at the increase of the service life of tools.

In practical use of the coated tool, however, we often encounter the debonding at the interface of the film and the tool material. It is important to grasp the behavior of the interface of the hard film and the tool material, to evaluate the precise interfacial strength.

Numerical simulations of the mechanical behavior of the materials coated by the hard film have been performed by many researchers. However, the deformation of the film on these analyses does not correspond to that of the actual hard film coated on the forging tool since the film itself is indented. Furthermore, because of the complete adhesion at the interface is postulated, the deterioration of the interface is not considered.

In the present paper, Finite element analysis for mechanical behavior of hard film - tool material interface of forging tool under a closer condition to an actual forging was performed by interface damage mechanics.

2. Examined model for interfacial behavior of coated forging tool

In the present study, we analyze the behavior of the interface between the hard film and the tool material by the examined model as shown in *Figure 1*. In this model, the hemispherical coated tool of 5mm in radius is indented to the workpiece of 20mm in diameter and 10 mm in height. The deformation of the bottom and the periphery of the workpiece are constrained.

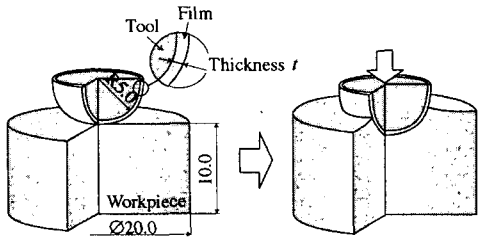

Figure 1: Schematic illustration of examined model.

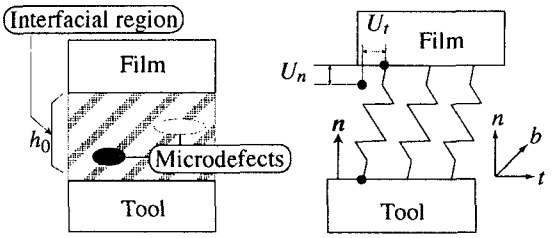

(a) Interfacial region (b) Equivalent spring model

Figure 2: Schematic illustrations of Interfacial region with microdefects.

3. Modeling of interface

Let us postulate the interfacial behavior occurs in the interfacial region shown in *Figure 2(a)*. In the interfacial region, microdefects develop when the external load is subjected, and the adhesion strength will be deteriorated.

In the present study, on calculating the interfacial behavior by the FEM, the adhesion of the interfacial region between the hard film and the tool materials is implemented by distributed non-linear springs as shown in *Figure2(b)*.

When the external load is applied, these points will produce an interfacial displacement $\boldsymbol{U}_{int}$. The interfacial displacement vector $\boldsymbol{U}_{int}$ can be expressed by the components of the normal direction n, tangential direction t and the other direction b according to a right hand Cartesian coordinate system in Figure2, as U_n, U_t and U_b

Then, we define the interfacial relative displacement $\boldsymbol{u}_{int}$ as follows:

$$\boldsymbol{u}_{int} = \left(u_n, u_t, u_b\right)^T = \frac{1}{h_0}\left(U_n, U_t, U_b\right)^T \tag{1}$$

where h_0 is the thickness of the interfacial region.

In the present study, we express the deterioration of the interface using the interfacial damage variable D_n.

The relation between the interfacial stress vector and the interfacial relative displacement can be obtained as follows:

$$\boldsymbol{T}_n = \left(1 - D_n\right)\boldsymbol{K}_{int}^0 \boldsymbol{u}_{int} \tag{2}$$

where $\boldsymbol{K}_n^0$ is the initial interfacial rigidity tensor at the intact state. We will adopt the following simple form:

$$\boldsymbol{K}_{int}^0 = \begin{pmatrix} K_n^0 & 0 & 0 \\ 0 & K_t^0 & 0 \\ 0 & 0 & K_b^0 \end{pmatrix} \tag{3}$$

The initial interfacial rigidity K_n^0, K_t^0 and K_b^0 are postulated to be expressed as follows:

$$K_n^0 = 2E_f E_t / \left(E_f + E_t\right), \quad K_t^0 = K_b^0 = 2G_f \cdot G_t / \left(G_f + G_t\right) \tag{4}$$

where E_f and E_t are the Young's moduli of the hard film and the tool materials, G_f and G_t are the their shear moduli.

Moreover, we define, for convenience, the thermodynamic conjugate force of the interfacial damage variable R_n as follows:

$$R_n \equiv \left\{ K_n^0 (u_n)^2 + K_t^0 (u_t)^2 + K_b^0 (u_b)^2 \right\} / 2 \tag{5}$$

The evolution equation of the interfacial damage variable D_n can be derived as follows:

$$\dot{D}_n = \frac{n_D}{S_D} \left\langle \frac{R_n - R_n^0}{S_D} \right\rangle^{n_D - 1} \left\langle \dot{R}_n \right\rangle \tag{6}$$

where n_D, S_D and R_n^0 are material constants.

The debonding is assumed to occur when the interfacial damage variable D_n attains the threshold damage variable D_{ncr}. When the debonding occurs, the interfacial rigidity is reduced to zero.

4. Finite element analysis of interfacial behavior

Figure 3 shows the discretized model, boundary conditions and the equivalent interfacial spring of the interface for the analysis. In the present study, the axisymmetric model is chosen.

The maximum indentation depth s_{max} is 4.5mm. For the parameter indicating the position of the interface, we adopt the angle θ (0-90°) as shown in *Figure 3*.

The commercial finite element code MARC2000 is used in the present study. The non-linear interfacial springs between the two material points on the opposite side of interface as shown in *Figure 3*, are implemented by use of the user subroutine equipped in the code.

For the friction condition, friction coefficient of $\mu = 0.3$ is employed by assuming the non-lubrication condition to promote the development of the interfacial damage variable.

We employ the following values, for the purpose of the elucidation of the characteristics of the proposed damage evolution equation qualitatively: n_D=2.0, S_D=50.0 and R_n^0=0.3.

5. Results and Discussion

Figure 4(a) and *4(b)* show the relation between the interfacial relative displacement u_n, u_t and the position of the interface θ with the parameter of the indentation depth s. As observed in *Figure 4(a)*, the interfacial relative displacement on normal direction u_n takes the maximum value at the position of θ=42°. This position is at the immediately behind the contact edge. The similar relation can be observed at any indentation depth.

On the other hand, the interfacial relative displacement on tangential direction u_t is distributed moderately. In any indentation depth, the maximum value of u_t is located

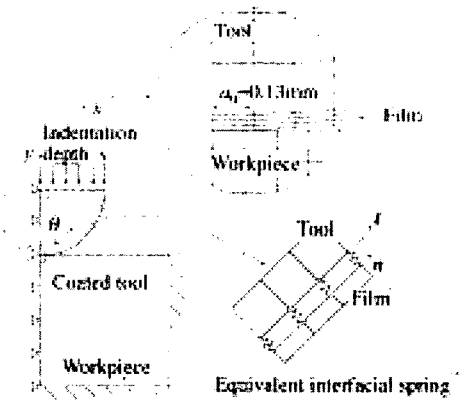

Figure 3: Analyzed model of indentation of hemispherical tool coated by hard film.

ahead of the contact edge.

Figure 5 shows the position of the maximum interfacial displacement on normal and tangential directions $u_{n,max}$ and $u_{t,max}$ at the indentation depth of s=2mm.

Figure 6 shows the change of the interfacial relative displacement u_n , u_t and the interfacial damage variable D_n to the indentation depth s, at the interfacial position of θ=45°. The interfacial damage variable D_n increases as the interfacial relative displacements increase. However, the development of D_n ceases after the interfacial relative displacements stop increasing.

6. Conclusions

In the present paper, FE analysis on the interfacial behavior of the indentation of the hemispherical tool coated by chromium electroplating to the workpiece is performed.

The results of the FE analysis show that the interfacial relative displacement in the normal direction takes its maximum value at the immediately back of the lip of the indentation in each indentation depth. On the other hand, the maximum value of the interfacial relative displacement in the tangential direction is located just ahead of the edge of the indentation.

References (omitted)

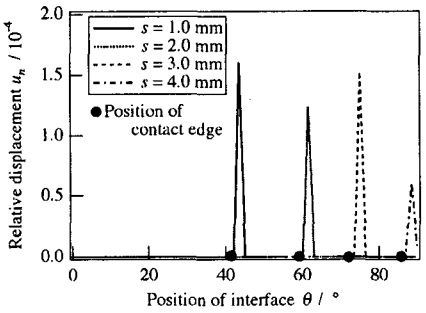

(a) Normal direction

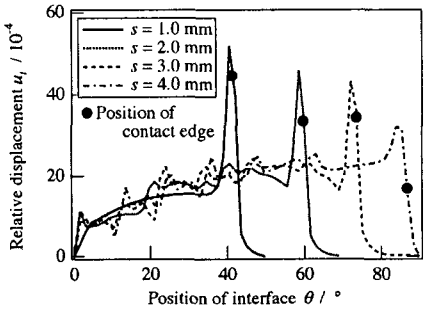

(b) Tangential direction

Figure 4: Effects of indentation depth on distribution of interfacial relative displacements u_n and u_t.

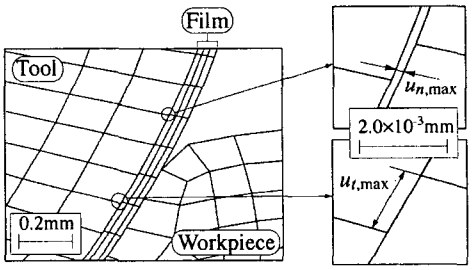

Figure 5: Position of maximum relative displacements $u_{n,max}$ and $u_{t,max}$ at indentation depth s=2mm.

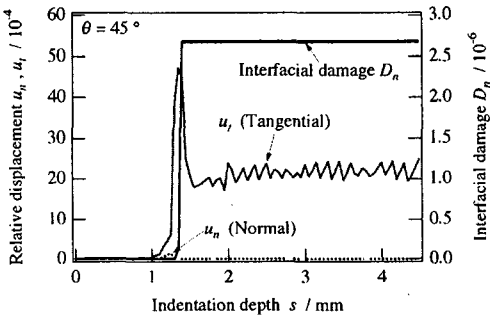

Figure 6: Change of relative displacement u_n, u_t and interfacial damage variable D_n to indentation depth s at interfacial position θ=45°.